01 Dec 2011

Pulmonary Diffusional Screening and the Scaling Laws of Mammalian Metabolic Rates

Chen Hou
Missouri University of Science and Technology, houch@mst.edu

Michael Mayo

Recommended Citation

C. Hou and M. Mayo, "Pulmonary Diffusional Screening and the Scaling Laws of Mammalian Metabolic Rates," *Physical Review E - Statistical, Nonlinear, and Soft Matter Physics*, vol. 84, no. 6, American Physical Society (APS), Dec 2011.
The definitive version is available at https://doi.org/10.1103/PhysRevE.84.061915

Pulmonary diffusional screening and the scaling laws of mammalian metabolic rates

Chen Hou
Department of Biological Sciences, Missouri University of Science and Technology, Rolla, Missouri 65409, USA

Michael Mayo*
Environmental Laboratory, US Army Engineer Research and Development Center, Vicksburg, Mississippi 39180, USA
(Received 2 November 2011; published 20 December 2011)

Theoretical considerations suggest that the mammalian metabolic rate is linearly proportional to the surface areas of mitochondria, capillary, and alveolar membranes. However, the scaling exponents of these surface areas to the mammals' body mass (approximately 0.9–1) are higher than exponents of the resting metabolic rate (RMR) to body mass (approximately 0.75), although similar to the one of exercise metabolic rate (EMR); the underlying physiological cause of this mismatch remains unclear. The analysis presented here shows that discrepancies between the scaling exponents of RMR and the relevant surface areas may originate from, at least for the system of alveolar membranes in mammalian lungs, the facts that (i) not all of the surface area is involved in the gas exchange and (ii) that larger mammals host a smaller effective surface area that participates in the material exchange rate. A result of these facts is that lung surface areas unused at rest are activated under heavy breathing conditions (e.g., exercise), wherein larger mammals support larger activated surface areas that provide a higher capability to increase the gas-exchange rate, allowing for mammals to meet, for example, the high energetic demands of foraging and predation.

DOI: 10.1103/PhysRevE.84.061915 PACS number(s): 87.19.Wx, 89.75.Da, 87.10.−e

I. INTRODUCTION

When mammals' locomotion status switches between rest and exercise, their oxygen uptake and metabolic rates increase, which scales with body mass. The resting metabolic rate (RMR) scales with a mammals' body mass m to a power of approximately $3/4$, RMR $\propto m^{3/4}$, over an astonishing seven orders of magnitude [1]. Recent studies with exercising mammals establish that an exercise metabolic rate (EMR) scales with m to a power of $7/8$, EMR $\propto m^{7/8}$, for body masses spanning a similar range, from 7 g to 500 kg [2,3]. These scaling relationships point to an incredible "economy of scale" [4]; in the resting state, a 10 000 fold increase in mass across mammalian species results in only a 1000 fold increase in the energy required to sustain an equivalent unit of mass. However, this phenomenon almost vanishes during exercise, more closely matching with intuition: as the number of a tissue's cells increase, the energy required to sustain them proportionally increases. This change in the scaling behavior of the metabolic rate during rest and exercise indicates that larger mammals have a larger capability to meet the increase in oxygen demand during aerobic exercise (e.g., running), by drastically increasing the oxygen uptake rate across the gas-exchange surface of alveolar membranes in the pulmonary acinus of the lung. There it binds with the hemoglobin of the red blood cells and is distributed to the rest of the body.

Several theoretical models have been proposed to obtain a better understanding of the mechanism underlying the scaling laws of the RMR and the EMR [3,5–7]. Aiming to explain the $3/4$ power law observed in mammals at rest, West *et al.* [7] hypothesized that the metabolic rate is proportional to the effective surface area across which the nutrients and energy exchanges occur, such as the capillary or mitochondrial surface areas, as opposed to the total area. In this model, the authors postulated that natural selection tends to maximize both internal efficiency and metabolic capacity by minimizing the scaling of transport distances and times, and scaling of exchange surface areas. Under these assumptions, the scaling exponent of the effective surface area was derived to be $3/4$. However, Weibel and Hoppeler later showed that the total volumes of mitochondrial and capillary erythrocytes, as well as their surface areas, scale almost linearly with body mass [3]. They suggested that surface area scaling exponents can explain the higher scaling of EMR, especially for athletic species [3]. So the seeming difficulty in explaining the $3/4$ and $7/8$ power laws for RMR and EMR, respectively, is that a theory based on first principles of optimization derives a $3/4$ scaling for effective surface area that directly leads to a $3/4$ scaling for basal metabolic rate (BMR), but the experimental data showed the surface areas of mitochondrial and capillary scale almost linearly with body mass; meanwhile, a theory based purely on the linear scaling of surface areas with body mass is able to explain the higher scaling powers for EMR, yet fails to address the $3/4$ power law for RMR.

This article bridges West *et al.*'s theory with Weibel and Hoppeler's data by offering a unifying physiological mechanism that may explain the discrepancy in the understanding between mammalian resting and exercise metabolic rate. The aerobic metabolic rate of a mammal is set by the capacity of the respiratory system to deliver oxygen to the blood within the pulmonary arteries, which involves surface areas in three main steps in the delivery process: (i) the effective surface of the alveolar membranes; (ii) the area of the muscle capillaries; and (iii) the area of the inner mitochondrial membrane [8]. These surface areas are effectively connected in series, and the oxygen uptake rates, both at rest and exercise, are constrained in particular by the alveolar membrane surface area, which is the primary focus of this paper.

*michael.l.mayo@usace.army.mil

II. METHODS

The uptake rate of oxygen by the total alveolar membranes lining the surface of the pulmonary acinus (in dimension of number of molecules per unit time) V_{O_2} can be modeled by [7]:

$$V_{O_2} = W \times S \times \Delta P, \tag{1}$$

wherein W is the permeability of membrane (in units of length per time), S is the surface area of the alveolar membranes in the lung, and ΔP is the partial pressure difference of oxygen across the membrane. For 36 species of mammals ranging in body mass from 2 g (Etruscan shrew) to 700 kg (cow), the total alveolar membrane surface area S was found to scale with body mass as $S \propto m^{0.95}$ [9,10].

The oxygen flux into the surface of alveolar membranes can be written as [11]

$$J = -\phi_W RT \beta_{O_2} D_{O_2} \frac{\Delta C}{\delta},$$

wherein ϕ_W is the volume fraction of water within the membranes; β_{O_2} and D_{O_2} are the Henry's law coefficient and the diffusion coefficient of oxygen in the membranes, respectively; R is the universal gas constant and T is the system (i.e., body) temperature; ΔC is the concentration difference of the respiratory gas across the membranes (for clarity, we will choose oxygen, O_2); and δ is the thickness of the membranes, which, at the level of the pulmonary acinus is roughly position independent. The membrane-plasma system can be effectively treated to good approximation as a water barrier, wherein ϕ_W, β_{O_2}, and D_{O_2} are calculated for water; we may then define a permeability (in units of length per time) for the alveolar membranes as

$$W = \frac{RT\beta_{O_2} D_{O_2}}{\delta} \propto \frac{1}{\delta}. \tag{2}$$

The geometry dependence of the permeability is therefore expressed with the membrane thickness. Early studies established that this thickness scales with body mass to an exponent of 0.05 [8,9]:

$$W \propto m^{-0.05}. \tag{3}$$

There is no evidence that ΔP scales with body mass during exercise [8,12]. Thus, Eq. (1) predicts that the oxygen uptake rate scales as $V_{O_2} \propto m^{0.9}$—a result consistent with the scaling law of the EMR described above, but not the RMR [1].

While the scaling exponent for the surface areas used in these estimates (0.95) is obtained from morphometric data for the total membrane surface area, several studies have demonstrated that mammals at rest use only a fraction of the (fixed) total alveolar membrane surface involved in pulmonary gas exchange [12–15]. The rest of the alveolar membranes are not active in the gas exchange; therefore, the effective surface area represented in Eq. (1)—the amount which actually contributes to the oxygen uptake rate—is smaller than the total, morphometrically derived, surface area. This is the diffusional screening phenomenon, which we briefly explain below.

A. The role of diffusional screening in respiratory gas exchange

Most gas exchange occurs within the pulmonary acinus [8,16], which connects to the bronchial tree at approximately the 15th branching bifurcation of the lung under resting conditions. An acinus is subdivided into eight subacini, defined as the airway trees beginning from the 18th branching bifurcation [8], wherein diffusion, rather than convection, serves as the dominant oxygen-transport mechanism. These remaining five generations of branching airways form a tree of alveolar ducts that support a system of alveoli lining the airways' surface; the membranes of the alveoli compose a surface in contact with respiratory gases permeable to O_2. Because of the arrangement of alveoli, the collective surfaces of all the lung's subacini form a highly convoluted, but space-filling, surface that allows for a maximum exchange area the size of a tennis court ($\approx$120 m^2) to be contained within the relatively small volume of mammalian pleural cavities.

In mammalian lungs, oxygen diffuses throughout the pulmonary subacinus under stationary conditions, where it eventually crosses the surface of alveolar membranes to reach, and bind with, the hemoglobin of the red blood cells [8]. As O_2 diffuses downstream within the subacinus, concentration gradients develop as progressively more O_2 molecules cross into pulmonary blood. The space-filling structure of the exchange surface enhances the concentration drop, because O_2 molecules have a high probability to be absorbed by the protruding surface regions, but only rarely penetrate into the deep fjord-like regions of the "crumpled" surface. This drop in O_2 concentration far from the respiratory bronchioles (the source of subacinar diffusion at rest, wherein the convection speed of oxygen falls below the diffusional speed) is referred to as diffusional screening [12–15].

B. Pulmonary efficiency of mammalian lungs

When exercise intensity increases, the resulting increase in ventilation pushes the diffusion source deeper into the system (from the 18th branch generation at rest, to about the 21st branch generation at heavy exercise), activating screened surface area and leading to an increase in the pulmonary efficiency η, which is the ratio of effective to total surface area [12,15]. The match between scaling exponents of the oxygen uptake rate during exercise and the total alveolar surface area indicates that the pulmonary efficiency η is nearly 100%, that is, the entire gas-exchange surface is active for highly aerobic conditions.

For mammals at rest however, η is generally less than 100%. Analytic models [15,17,18] and computer simulations of two-dimensional surfaces [12,14] show that pulmonary efficiency decreases as the size of the acinus increases—a result attributed to the larger surface areas provided by the increased size of the airway trees defined by the shallow onset of gas diffusion in the lung at rest. Larger mammals usually have larger acini, so that if η obeys a scaling law, it should scale with body mass negatively at resting conditions. Taking these factors into account, Eq. (1) becomes

$$V_{O_2} = W \times \eta \times S \times \Delta P, \tag{4}$$

wherein $\eta \times S$ gives the area of unscreened or active membrane surface area. The main insight of Eq. (4) is that the negative scaling exponent of η provides a way to explain why the scaling exponent of V_{O_2} at rest (0.75) is lower than the one of total alveolar membrane surface area (0.95).

Sapoval *et al.* estimated the scaling relationship between mammalian pulmonary efficiency and body mass by computer simulation using structural data for mouse, rat, rabbit, and human pulmonary acini, finding the efficiency to scale approximately as $\eta \propto m^{-0.16}$ [12]. But, as the authors admitted, the efficiency is computed according to a two-dimensional Hilbert geometry. Moreover, their analyses provided only four data points, which are not enough to provide an accurate estimate to the power-law relationship. We extend these analyses by using a realistic, three-dimensional analytic model of the gas-exchange process recently developed by Hou *et al.* [15], which is established upon first principles of oxygen transportation and uptake, while also utilizing a broader range of current experimental data on mammalian lungs to infer a scaling law for pulmonary efficiency.

III. RESULTS

The validity of Hou's model was established using measured transport and structural parameters for the human lung, giving predictions of the oxygen uptake rate for different breathing conditions, such as different levels of aerobic exercise, agreeing with measured values to within a few percent. The model also predicts that, at rest, the pulmonary efficiency can be expressed as

$$\eta = \eta_0 \times d/(W \times S_a),$$

wherein η_0 is a normalization constant independent of body mass, d is the diameter of the terminal bronchiole, W is the permeability of the alveolar membranes, and S_a is the total surface area of a typical pulmonary acinus. Since the lung is a space-filling network composed of alveoli, it can be treated as a set of cubes (a similar space-filling structure), wherein the length of each cube l is matched to the smallest geometric scale in the lung—the diameter of an alveolus. The number of alveoli that can fill a single acinus is therefore proportional to $(L/l)^3$, wherein L is the diameter of an average acinus. As surface area of each alveolus is proportional to l^2, it follows that the surface area of an acinus S_a is proportional to $(L/l)^3 \times l^2 = L^3/l$. Substituting this result into the equation above gives

$$\eta = \eta_0 \times d \times l/(W \times l^3), \tag{5}$$

wherein η_0 is a proportionality constant.

In Eq. (4) the permeability scales as $W \propto m^{-0.05}$ [9] as explained above; for the other three structural parameters (the diameter of terminal bronchiole d, the diameter of an acinus L, and the diameter of an alveolus l) we compiled morphometric data available from literature sources that includes 16 species of mammals with body masses ranging from 6 g (Harvest Mouse) to 74 kg (Human), from which we obtained the following scaling relations: $L = 0.042 \times m^{0.172}$ [$R^2 = 0.96$; 95% CI = (0.13, 0.21)] (Fig. 1); $d = 0.0052 \times m^{0.21}$ [$R^2 = 0.72$; 95% CI = (0.12, 0.30)] (Fig. 2); $l = 0.0031 \times m^{0.151}$ [$R^2 = 0.66$; 95% CI = (0.09, 0.22)] (Fig. 3). Tables I, II, and III provide the source data used in these figures.

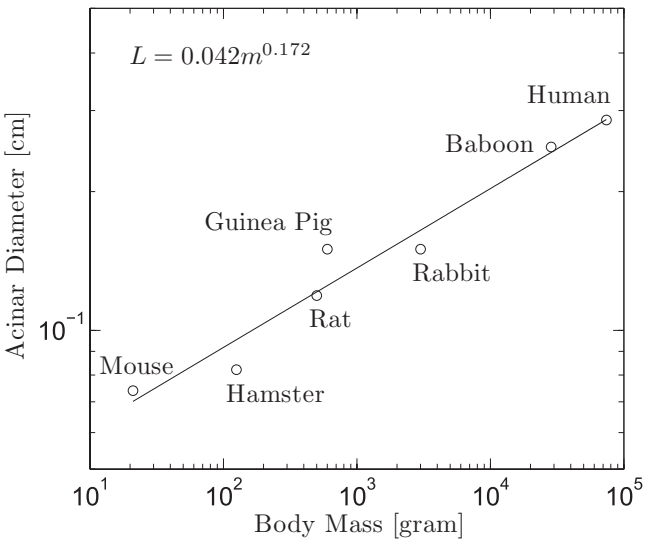

FIG. 1. Scaling relationship between the diameter of an acinus L and body mass.

Although these scaling laws were obtained empirically, directly from the experimental data, the scaling exponents for d and L are not, in principle, independent of one another. At the terminal bronchiole, the dominant oxygen-transport mechanism changes from convection to diffusion, so that the flow velocity is roughly equal to the diffusion velocity [12]; the diffusion velocity is proportional to D/L [12], wherein D is the diffusion coefficient of oxygen in air. The flow velocity at the terminal bronchiole v can be determined through mass conservation (i.e., a continuity equation at constant fluid density): $u_0 = (\pi/4) \times v \times N \times d^2$, wherein u_0 is the volume flow at trachea (volume per unit time), and N is the total number of acini in the lung. Since the volume of an acinus is proportional to L^3, the total volume of a mammalian lung

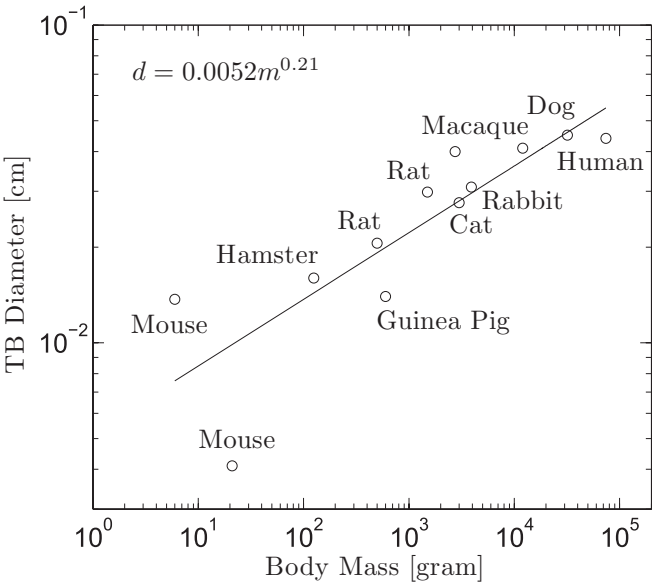

FIG. 2. Scaling relationship between the diameter of a terminal bronchiole (TB) d and body mass.

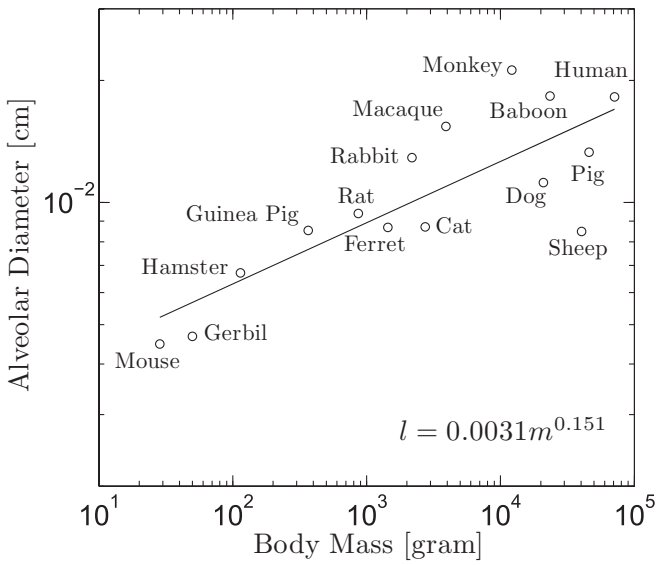

FIG. 3. Scaling relationship between the diameter of an alveolus l and body mass.

V_{lung} is proportional to $N \times L^3$. Thus L and d are related by

$$D/L \propto u_0 \times L^3/(V_{\text{lung}} \times d^2). \tag{6}$$

Here the total lung volume scales as $V_{\text{lung}} \propto m^{1.05}$, and volume flow at the trachea scales as $u_0 \propto m^{0.8}$ [1].

Following Eq. (6), the scaling exponents of the acinar diameter α_L and the transitional bronchiole diameter α_d are approximately related by $4\alpha_L = 0.25 + 2\alpha_d$—a result confirmed by Figs. 1 and 2 (i.e., $4 \times 0.172 = 0.688 = 0.250 + 2 \times 0.210 = 0.670$). Substituting these scaling laws into Eq. (5) yields

$$\eta \propto \eta_0 \times m^{0.21} \times (m^{0.151}/m^{-0.05})/m^{3\times 0.172},$$

from which it follows that

$$\eta \propto \eta_0 \times m^{-0.1}. \tag{7}$$

We should emphasize that the alveoli and acini are assumed here to be cube shaped, and that the bronchiole cross section is considered to be square, so detailed physiological information of the normalization coefficient η_0 is not captured by the model. Therefore, the scaling argument used to arrive at Eq. (7) should not be used to directly calculate the actual efficiency of the lung. Rather, the key assumption here is that the scaling relationships between the cube-based model of Hou *et al.* and the actual mammalian physiology are only equivalent up to a constant.

TABLE I. Diameter of an acinus L and body mass. Data used in Fig. 1.

Species	Body Mass (g)	L (cm)	Reference
Mouse	21	0.074	[12]
Hamster	125	0.082	[20]
Rat	500	0.119	[21]
Guinea Pig	600	0.150	[22]
Rabbit	3 000	0.150	[21]
Babooon	28 500	0.250	[22]
Human	74 000	0.286	[23]

TABLE II. Diameter of a terminal bronchiole (TB) d and body mass. Data used in Fig. 2.

Species	Body Mass (g)	d (cm)	Reference
Harvest Mouse	6	0.0137	[24]
Mouse	21	0.0041	[25–28]
Hamster	125	0.0160	[20]
Rat	500	0.0206	[21]
Guinea Pig	600	0.0140	[29]
Giant Pouched Rat	1 500	0.0298	[24]
Cat	2 750	0.0400	[30]
Rabbit	3 000	0.0276	[21]
Long-Tail Macaque	3 917	0.0309	[31]
Pigtail Macaque	12 000	0.0410	[32]
Dog	32 000	0.0450	[33]
Human	74 000	0.0440	[23]

IV. DISCUSSION

This negative scaling exponent of the pulmonary efficiency at rest, $\eta \propto m^{-0.1}$, qualitatively explains why $V_{O_2} \propto m^{0.75}$ does not match $S \propto m^{0.95}$. However, in light of Eq. (4), there remains a mismatch of approximately 0.05 in the scaling exponents (i.e., $0.75 \neq -0.05 - 0.10 + 0.95 = 0.80$). This could be attributed to a slightly negative scaling exponent for the partial pressure difference of oxygen across the alveolar membranes (i.e., $\Delta P \propto m^{-0.05}$).

This idea is not without precedent. Weibel first introduced it in his celebrated book [8], but also pointed out that estimating ΔP depends on information regarding pulmonary blood flow, the O_2 binding properties of blood (e.g., hemoglobin saturation kinetics), and the pulmonary diffusion capacity. However, independent theoretical considerations [5] show that ΔP scales with a power of approximately -0.05, which,

TABLE III. Diameter of an alveolus l and body mass. Data used in Fig. 3.

Species	Body Mass (g)	l (cm)	Reference
Harvest Mouse	28.5	0.004 48	[12,22,34,35]
Gerbil	50	0.004 68	[34]
Hamster	114	0.006 71	[34,35]
Rat	366	0.008 53	[22,34,35]
Guinea Pig	867	0.009 40	[22,34,36]
Ferret	1 440	0.008 68	[34]
Cat	2 180	0.012 90	[34,37]
Rabbit	2 738	0.008 71	[12,34,35]
Long-Tail Macaque	3 917	0.015 40	[34]
Monkey	12 150	0.021 20	[34]
Dog	20 900	0.011 20	[34]
Baboon	23 450	0.018 30	[22,35]
Sheep	40 400	0.008 48	[34,36]
Pig	45 900	0.013 30	[34]
Human	71 160	0.018 20	[12,35]

if confirmed by experiments, would completely eliminate the discrepancy in the scaling exponents of Eq. (4) (i.e., $0.75 = -0.05 - 0.10 + 0.95 - 0.05 = 0.75$).

In the mammalian pulmonary system, the space-filling alveolar membranes, wherein the oxygen diffusion occurs, are coupled with the branching pulmonary vascular system, wherein oxygen perfusion occurs. These two systems constrain each other and both control the oxygen supply. The inclusion of a diffusional screening mechanism into a conceptual description of mammalian lungs implies that at rest only a fraction of pulmonary capillaries be closed and inactive for the oxygen transfer, so that diffusion and perfusion match. Numerous experimental studies have shown that more than half of the pulmonary capillaries in the human lung are closed under resting conditions, and most of them are opened during exercise [19]. The recruitment of pulmonary capillaries, which is an adaptive mechanism similar to that of the alveolar membranes, is believed to be the main mechanism to satisfy the increase of oxygen demand during exercise [19]. This may be also true for other mammalian lungs.

The empirical data compiled by Weibel and Hoppeler [3] shows that total capillary volume scales with body mass to a power of 0.98, contradictory to the theoretical prediction of West *et al.* (0.75) [5]. However, the 3/4 scaling exponent for the capillary number derived by West *et al.* stems from optimization, in which the energy dissipation in the vascular system of resting mammals is minimized. This scaling exponent therefore may be reflective of the exponent for opened or active capillary number at rest, instead of the one for total, morphometrically derived, capillary number. This mismatch in scaling exponents between capillary number and West *et al.*'s result may be dismissed in the future if empirical measurements confirm that the fraction of closed capillaries at rest increases with body mass systematically, and that all capillaries are open during aerobic exercise, similar to the pattern observed for the alveolar membranes.

V. CONCLUSIONS

Under heavy exercise, the efficiency of the lung as a gas exchanger nears 100%, wherein the oxygen uptake rate across the total surface of alveolar membranes was shown to scale with body mass as $V_{O_2} \propto m^{0.9}$ [Eq. (1)], which is consistent with the results of current experiments. By contrast, strong theoretical arguments and many experimental data show that this oxygen uptake rate scales quite differently at rest than exercise, $V_{O_2} \propto m^{0.75}$. As we have shown, it may be possible to reconcile this disparity for mammals by including the fact that rest and exercise represent differing levels of pulmonary efficiency. These considerations lead to a resting pulmonary efficiency that scales negatively with overall body mass, $\eta \propto m^{-0.1}$, indicating that screening of respiratory gases from the pulmonary gas-exchange surface of alveolar membranes in mammalian lungs could be the determining reason for the mismatch between mammalian resting and exercise metabolic rates.

ACKNOWLEDGMENTS

This work was partially supported by the US Army's Environmental Quality and Installations 6.1 basic research program. We thank P. Pfeifer for insightful discussions and helpful advice. The Chief of Engineers approved this material for publication.

APPENDIX: EXPERIMENTAL DATA

Data was compiled from literature sources and used to identify the scaling relationships presented in Figs. 1, 2, and 3. This source data is presented in Tables I, II, and III, respectively. Where more than one source is cited, an arithmetic average of the reported mean values was used. Minimization of a least-squares functional was used to fit the data to a power-law relationship; R^2 and confidence intervals (95% CIs) are reported for these data in the main text.

[1] R. Peters, *The Ecological Implications of Body Size* (Cambridge University Press, Cambridge, 1986).
[2] C. Bishop, Proc. R. Soc. London **266**, 2275 (1999).
[3] E. Weibel and H. Hoppeler, J. Exp. Biol. **208**, 1635 (2005).
[4] L. Bettencourt, J. Lobo, D. Helbing, C. Khnert, and G. West, Proc. Natl. Acad. Sci. USA **104**, 7301 (2007).
[5] G. West, J. Brown, and B. Enquist, Science **276**, 122 (1997).
[6] J. Banavar, A. Maritan, and A. Rinaldo, Nature (London) **399**, 130 (1999).
[7] G. West, J. Brown, and B. Enquist, Science **284**, 1677 (1999).
[8] E. Weibel, *The Pathway for Oxygen* (Harvard University Press, Boston, MA, 1984)
[9] P. Gehr, D. Mwangi, A. Ammann, G. Maloiy, C. Taylor, and E. Weibel, Respir. Physiol. **44**, 61 (1981).
[10] E. Weibel, Ann. Rev. Physiol. **49**, 147 (1987).
[11] A. Katchalsky, *Biophysics and Other Topics: Selected Papers* (Academic, New York, 1976).
[12] B. Sapoval, M. Filoche, and E. Weibel, Proc. Natl. Acad. Sci. USA **99**, 10411 (2002).
[13] M. Felici, M. Filoche, C. Straus, T. Similowski, and B. Sapoval, Resp. Physiol. Neurobiol. **145**, 279 (2005).
[14] C. Hou, S. Gheorghiu, M.-O. Coppens, V. Huxley, and P. Pfeifer, in *Fractals in Biology and Medicine*, edited by G. Losa, D. Merlini, T. Nonnenmacher, and E. Weibel (Birkhäuser, Basel, 2005), pp. 17–30.
[15] C. Hou, S. Gheorghiu, V. Huxley, and P. Pfeifer, PLoS Comp. Biol. **6**, e1000902 (2010).
[16] B. Haefeli-Bleuer and E. Weibel, Anat. Rec. **220**, 401 (1988).
[17] D. S. Grebenkov, M. Filoche, B. Sapoval, and M. Felici, Phys. Rev. Lett. **94**, 050602 (2005).
[18] M. Mayo, Ph.D. thesis, University of Missouri, 2009.
[19] C. Hsia, Chest **122**, 1774 (2002).
[20] A. R. Kennedy, A. Desrosiers, M. Terzaghi, and J. B. Little, J. Anat. **125**, 527 (1978).
[21] M. Rodriguez, S. Bur, A. Favre, and E. Weibel, Am. J. Anat. **180**, 143 (1987).
[22] F. Miller, R. Mercer, and J. Crapo, Aerosol Sci. Technol. **18**, 257 (1993).

[23] E. Weibel, B. Sapoval, and M. Filoche, Resp. Physiol. Neurobiol. **148**, 3 (2005).
[24] R. Gomes and J. Bates, Resp. Physiol. Neurobiol. **130**, 317 (2002).
[25] H. Obara, M. Sekimoto, and S. Iwai, Thorax **34**, 479 (1979).
[26] A. T. Have-Opbroek, Anat. Embryol. **174**, 49 (1986).
[27] R. W. Amy, D. Bowes, P. H. Burri, J. Haines, and W. M. Thurlbeck, J. Anat. **124**, 131 (1977).
[28] A. Braun, H. Ernst, H. Hoymann, and S. Rittinghausen, in *The Laboratory Mouse*, edited by H. Hedrich and G. Bullockl (Academic, New York, 2004), pp. 17–30.
[29] J. Schreider and J. Hutchens, Anat. Rec. **196**, 313 (1980).
[30] T. G. Klingele and N. C. Staub, J. Appl. Phys. **30**, 224 (1971).
[31] A. Hislop, S. Howard, and D. Fairweather, J. Anat. **138**, 95 (1984).
[32] E. Boyden, Anat. Rec. **186**, 15 (1976).
[33] K. Horsfield and G. Cumming, Resp. Physiol. **173**, 173 (1976).
[34] H. Lum and W. Mitzner, J. Appl. Phys. **62**, 1865 (1987).
[35] R. R. Mercer, M. L. Russell, and J. D. Crapo, J. Appl. Physiol. **77**, 1060 (1994).
[36] S. M. Tenney and J. E. Remmers, J. Appl. Phys. **21**, 1328 (1966).
[37] T. G. Klingele and N. C. Staub, J. Appl. Phys. **28**, 411 (1970).